

Supporting Information for the article: "Spectral Shaping by Radiative Energy Transfer in CsPbBr₃ Nanocrystal - Dye Mixtures"

Ina Flaucher^{*,1,2}, Marco van der Laan¹, Jef Huisman², Peter Schall^{*,1}

¹ Institute of Physics, University of Amsterdam, Amsterdam, 1098 XH, The Netherlands

² Department of Freshwater and Marine Ecology, Institute for Biodiversity and Ecosystem Dynamics, University of Amsterdam, Amsterdam, 1098 XH, The Netherlands

Corresponding authors: i.j.flaucher@uva.nl, p.schall@uva.nl

Chemicals and Materials

Lead (II) bromide (PbBr₂, 99 %), cesium carbonate (Cs₂CO₃, 99 %), 1-octadecene (ODE, technical grade 90 %), oleic acid (OA, technical grade 90 %), oleylamine (OAm, 90 %) and 'Nile Red powder for microscopy' were all purchased from Sigma Aldrich and used as received. Toluene (99.5 %) was purchased from VWR.

Synthesis of CsPbBr₃

The synthesis of the CsPbBr₃ nanocrystals was performed according to Protesescu et al.¹, with minor modifications. First, Cs-oleate was prepared by adding 814 mg Cs₂CO₃ into a 100 mL flask along with 40 mL ODE and 2.5 mL OA. This mixture was degassed for 1 h and subsequently heated to 150 °C under N₂ until all precursors were dissolved and the solution became transparent.

In a second flask 30 mL ODE and 690 mg PbBr₂ were degassed under N₂ at 120 °C for 30 min. Then, 5 mL OAm and 5 mL OA (degassed for 30 min) were injected with a syringe into the second flask and the temperature was raised to 160 °C until all the PbBr₂ was dissolved. The Cs-oleate was reheated to 100 °C and degassed for 30 min. Then 4 mL Cs-oleate were quickly injected into the 160 °C PbBr₂ solution with a syringe. The reaction was quenched after 5 s with an ice water bath. Purification was performed in three cycles of centrifugation at 5krpm and redispersion of the nanocrystals in toluene. The supernatants resulting of the first two centrifugation cycles were discarded, while the precipitates were redissolved. The supernatant resulting from the third cleaning cycle was used as a basis for all experiments in the study.

Data processing

ODs were derived from the experimentally measured transmission spectra via:

$$OD(\lambda) = -\log_{10} \frac{T_s(\lambda)}{T_0(\lambda)}, \quad (S1)$$

with $T_0(\lambda)$ being the fractional transmission through a quartz cuvette filled with toluene and $T_s(\lambda)$ being the transmission through the cuvette filled with either or both of the materials.

Lifetime data were normalised to their respective maximum

Radiative versus non-radiative energy transfer

To further substantiate the absence of non-radiative energy transfer, we estimate (i) the diffusion time of the particles, and (ii) the full distribution of nanocrystal-dye distances.

(i) Diffusion time

The Stokes-Einstein equation for diffusion is given by

$$D = \frac{k_B T}{6\pi\eta r}, \quad (\text{S2})$$

where

- Temperature: $T = 294 \text{ K}$
- Dynamic viscosity (Toluene): $\eta = 0.56 \times 10^{-3} \text{ Pa s}$
- Particle radii:
 - Nanocrystals: $r = 5 \text{ nm}$
 - Nile Red: $r = 0.5 \text{ nm}$

From this information, the diffusion coefficients are calculated as: $D_{\text{nanocrystals}} = 3.69 \times 10^{-11} \text{ m}^2/\text{s}$ and $D_{\text{Nile Red}} = 3.69 \times 10^{-10} \text{ m}^2/\text{s}$. The diffusion time t of the faster component (Nile Red) for an average interparticle distance of $L = 20.8 \text{ nm}$ is estimated by

$$t = \frac{L^2}{D_{\text{Nile Red}}}. \quad (\text{S3})$$

This results in an estimated diffusion time of $t \approx 1.2 \mu\text{s}$, which is the time required for the particles to diffuse over their interparticle distances.

(ii) Distance distribution

Sufficiently short distances for non-radiative energy transfer may still occur in the instantaneous distribution of the particles. To elucidate this possibility, we generated random spatial distributions of nanocrystals and dye molecules in the computer, and used those to extract the distribution of nanocrystal-dye distances, which we show in Fig. S1. Efficient Förster energy transfer can occur up to distances of $\sim 8 \text{ nm}$, which we have highlighted in grey. From this distribution, we see that only a very small fraction ($\sim 3\%$) of nanocrystal-dye pairs are within the required distance for non-radiative transfer, while, as we can see from Fig.1 in the main text, the chances of Nile Red (re-)absorbing green light is $\sim 90\%$. We thus conclude that, while some rare non-radiative energy transfer may occur, its contribution is minor compared to that of radiative transfer, consistent with the observed PL lifetime reported in the main text.

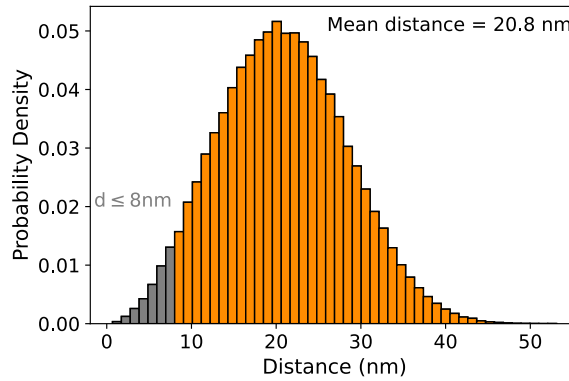


Figure S1: **Distribution of nanocrystal-dye distances.** The distribution was computed for the densities of nanocrystals and dye molecules in our suspension, assuming a random distribution of the fluorophores.

Photon Random Walk Model

Simulated data presented in the figures of the main text were constructed using a photon tracing, or photon random walk, model. In the model, experimental transmittance, excitation and photoluminescence data was used to trace the positions and wavelengths of photons through a 2D simulated cuvette filled with CsPbBr₃, Nile Red or mixtures thereof. These simulations explicitly incorporate the effects of photon absorption and emission by the medium to model radiative energy transfer between the two compounds and its result on the output photoluminescence spectra for any given set of parameters. A random walk model enables this by treating the underlying spectra of excitation, transmission and photoluminescence as probability distributions from which weighted numbers can be drawn. These numbers, representing photon position and wavelength, are propagated through the simulation and, by running sufficient amounts of photons, the outcomes of simulated experiments are modelled. In this way, complex processes can be simulated even if the underlying analytical equations are not easily solvable. The modelled processes are detailed in the following subsections.

Simulated Geometry

The simulations are run in a 2D square box with an edge size of 1 cm, equal to the the size of cuvettes used in the experiments. The inside of the box is filled with the light-interacting medium and the outside is air or vacuum. Photons ending up outside this box are counted as detected and cannot re-enter the box again. Since photons are detected on all sides of this box, this situation resembles an integrating sphere.

Excitation

Photons are initialized in the simulation by directing them at an angle normal to the 'bottom' boundary of the box. The wavelengths of these photons are randomly drawn from the spectrum of the lamp used in the integrating sphere measurements, from an AM 1.5G spectrum or from a Gaussian lineshape centered around some chosen wavelength, depending on the simulation.

Reflection

Photons impinging on a boundary of the simulated box have a chance of being reflected or transmitted based on the Fresnel equations for reflection. Here, the equations are dependent on the refractive index of the media, 'n' ($n = 1.5$ inside the box and $n = 1$ outside the box) and on the angles under which the photons arrive at the boundary. The light is assumed to be completely unpolarized and wavelength dependence of the refractive indices is not taken into account. If the initialized photons end up in the box, they have a chance to interact with the medium.

Transmittance and Photon Step-size

Whether or not photons are transmitted through the medium is determined in the simulation by a photon step-size extracted from the transmittance spectrum of a mixture of CsPbBr₃ and Nile Red of some arbitrary concentration. The mixture transmittance is constructed by adding the experimental optical densities of individual CsPbBr₃ and Nile Red according to,

$$OD_{Mix}(\lambda) = c_1 * OD_{NC}(\lambda) + c_2 * OD_{NR}(\lambda) \quad (S4)$$

Here, $OD_{NC}(\lambda)$ and $OD_{NR}(\lambda)$ are the wavelength-dependent optical densities from CsPbBr₃ and Nile Red as obtained from experimental transmittance measurements and converted according to Eq. S1. The pre-factors c_1 and c_2 allow for constructing arbitrary concentration mixtures. The constructed optical density of the mixture allows for defining a step-size of photons called the mean-free path length according to Eqs. S1, S4 and,

$$l_{mfp}(\lambda) = \frac{-d}{\ln(T_{Mix}(\lambda))} \quad (S5)$$

Here, $l_{mfp}(\lambda)$ is the mean-free path length of photons of wavelength ' λ ' and ' $T_{Mix}(\lambda)$ ' is the transmittance spectrum of the mixture for a cuvette of length ' d '.

Technically the free path length of photons lie on an exponential distribution but in these simulations photons always have a step-size equal to the mean of that distribution. Thus, photons in the simulation always travel a distance equal to the mean-free path length after which they interact with the medium. If photons hit a boundary within that travelling distance then the Fresnel equations determine whether photons are reflected back into the medium, and travel the remaining distance, or leave the simulation.

Absorption and Scattering

After travelling a distance of l_{mfp} , and if photons are still within the medium, photons have a chance to be either absorbed or scattered by either CsPbBr₃ or Nile Red. These relative probabilities of absorption by material 1 or 2, ' P_{A1} ', ' P_{A2} ' and scattering, ' P_{S1} ', ' P_{S2} ' are determined from the experimental transmittance spectra of CsPbBr₃ and Nile Red by fitting the spectra, with a polynomial function, at wavelengths longer than the known bandgap or lowest energy transition of these materials. Since no absorption is expected for these longer wavelengths, and reflection is accounted for, it is assumed that any drop in transmittance at these wavelengths is caused purely by scattering. From these fits an optical density purely attributed to absorption OD_A or scattering OD_S can be constructed and thus the relative probability of absorption and scattering on material 1 or 2 is defined as,

$$P_i = \frac{OD_i}{OD_{A1} + OD_{S1} + OD_{A2} + OD_{S2}} \quad (S6)$$

These relative probabilities for each event ' P_i ' are wavelength-dependent and a draw of random numbers in the simulations determines which of these events takes place. After a scattering event the angle of trajectory of a photon is uniformly chosen from $0 - 2\pi$, while the photons' wavelength, and therefore the magnitude of the next step, remains unchanged.

Emission

After an absorption event by either material 1 or material 2 photons have a chance to be re-introduced in the simulation based on the, experimentally determined, photoluminescence quantum yields of the two materials, ' QY_1 ' and ' QY_2 '. A random number is drawn and compared with the quantum yield to determine whether a photon is re-introduced. If re-emission occurs then the photon is given a new random angle of direction of travel between $0 - 2\pi$ and a new wavelength. The new wavelength is drawn from the experimental photoluminescence spectra of CsPbBr₃ and Nile Red, weighted by the PL intensity and depending on which material the photon was absorbed in.

The simulations enforce energy conservation by demanding that the probability for emitting photons above the absorbed photon's energy plus 25 meV is zero.

Multiple cycles and termination

Thus by repeated steps taken by the photons they diffuse through the simulated cuvette. The subsequent absorption and emission events allow for radiative energy transfer within the same material and between the two materials. The simulation is run in parallel for multiple photons and is terminated once all photons have left the boundaries of the box or have been absorbed but not re-emitted.

Types of simulations

Transmittance spectra of mixtures are simulated by running a full simulation but only counting photons as 'detected' if they escape the boundary opposite of the incident boundary under a narrow angle. Full (photoluminescence) spectra are simulated by counting all photons, independent of crossed boundary, as 'detected'. To construct photoluminescence excitation spectra or the relative shaping efficiencies simulations are run with excitation spectra with a Gaussian lineshape and counting photons leaving from all boundaries and processing these results according to the equations detailed in the subsequent section.

Definitions of Shaping Efficiencies

Shaping efficiency:

$$SE = \frac{\int_{560}^{700} I_{shaped,mix}(\lambda) d\lambda}{\int_{560}^{700} I_{in}(\lambda) d\lambda} \quad (S7)$$

Relative gain in shaping efficiency:

$$rSE = \frac{\int_{560}^{700} I_{shaped,mix}(\lambda) d\lambda - \int_{560}^{700} I_{shaped,NR}(\lambda) d\lambda}{\int_{560}^{700} I_{in}(\lambda) d\lambda} \quad (S8)$$

Monochromatic shaping efficiency:

$$rSE_{mono} = \frac{\int_{560}^{700} I_{shaped,mix}(\lambda) d\lambda - \int_{560}^{700} I_{shaped,NR}(\lambda) d\lambda}{\int I_{in}(\lambda) d\lambda} \quad (S9)$$

Figures

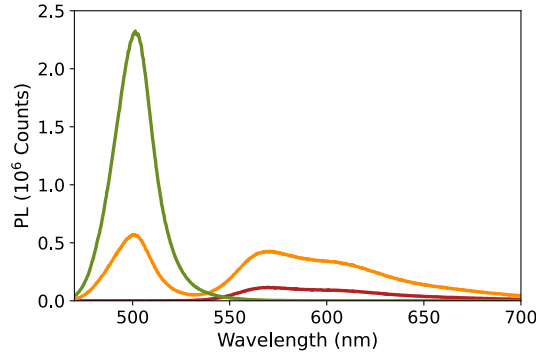


Figure S2: **Raw Photoluminescence Spectra.**

Raw PL spectra of the CsPbBr₃ nanocrystals (green) , the Nile Red dye (red), and their mixture (orange), taken at excitation wavelength of 400nm.

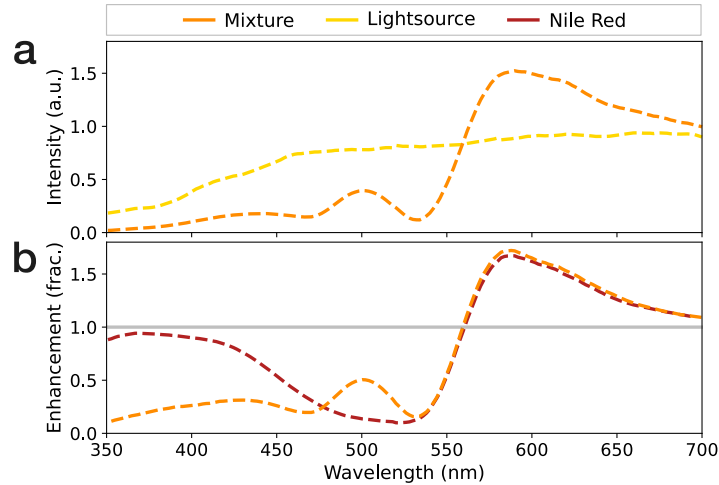


Figure S3: **Photon random walk model, AM1.5G.** (a) Simulated spectral modifications (orange curve) on the AM1.5G solar spectrum (yellow curve) upon interaction with the mixture at 1:1 concentration ratio and the experimental PLQY values. (b) Simulated enhancement ratio of the pure Nile Red sample (red) and the mixture (orange).

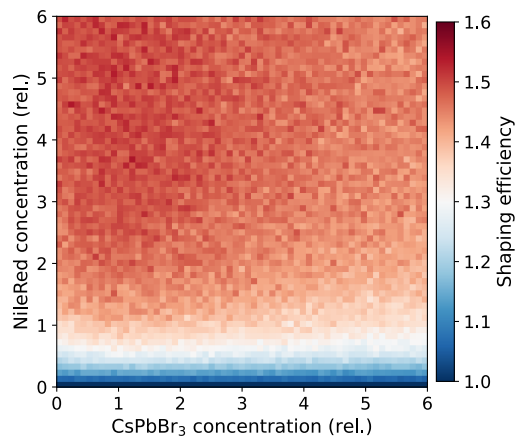


Figure S4: Simulated shaping efficiencies of the material mixture upon interaction with the AM1.5G solar spectrum. Concentrations of 1 benchmark the experimental inputs.

References

- (1) Protesescu, L.; Yakunin, S.; Bodnarchuk, M. I.; Krieg, F.; Caputo, R.; Hendon, C. H.; Yang, R. X.; Walsh, A.; Kovalenko, M. V. Nanocrystals of Cesium Lead Halide Perovskites (CsPbX_3 , $X = \text{Cl, Br, and I}$): Novel Optoelectronic Materials Showing Bright Emission with Wide Color Gamut. *Nano Letters* **2015**, *15*, 3692–3696, DOI: 10.1021/nl5048779.

	Positive	Negative	Net
NC QY = 0.0			
WL range	-	300-520 nm	-
% of Phots.	0%	58%	-
Rel. SE	0.0%	-6.3%	-6.3%
NC QY = 0.1			
WL range	300 - 385 nm	385 - 520 nm	-
% of Phots.	3%	55%	-
Rel. SE	0.0%	-4.8%	-4.8%
NC QY = 0.2			
WL range	300 - 420 nm	420 - 520 nm	-
% of Phots.	14%	44%	-
Rel. SE	0.4%	-4.0%	-3.6%
NC QY = 0.3			
WL range	300 - 430 nm	430 - 520 nm	-
% of Phots.	17%	41%	-
Rel. SE	1.2%	-3.2%	-2.0%
NC QY = 0.4			
WL range	300 - 440 nm	440 - 520 nm	-
% of Phots.	21%	37%	-
Rel. SE	2.0%	-2.5%	-0.5%
NC QY = 0.5			
WL range	300 - 445 nm	445 - 520 nm	-
% of Phots.	24%	34%	-
Rel. SE	3.0%	-2.1%	0.9%
NC QY = 0.6			
WL range	300 - 455 nm	455 - 520 nm	-
% of Phots.	28%	30%	-
Rel. SE	4.1%	-1.6%	2.5%
NC QY = 0.7			
WL range	300 - 460 nm	460 - 520 nm	-
% of Phots.	30%	28%	-
Rel. SE	5.3%	-1.2%	4.1%
NC QY = 0.8			
WL range	300 - 465 nm	465 - 520 nm	-
% of Phots.	33%	25%	-
Rel. SE	6.5%	-0.9%	5.6%
NC QY = 0.9			
WL range	300 - 470 nm	470 - 520 nm	-
% of Phots.	35%	23%	-
Rel. SE	7.8%	-0.6%	7.2%
NC QY = 1.0			
WL range	300 - 475 nm	475 - 520 nm	-
% of Phots.	37%	21%	-
Rel. SE	9.2%	-0.4%	8.8%

Table S1: Relative shaping efficiencies using the AM 1.5G spectrum for varying nanocrystal (NC) quantum yields (QY)